Int. J. Heat Mass Transfer. Vol. 26, No. 6, pp. 815-822, 1983
Printed in Great Britain

0017-9310/83/060815-08 $03.00/0

NATURAL CONVECTION HEAT TRANSFER IN A POROUS LAYER WITH INTERNAL FLOW OBSTRUCTIONS

ADRIAN BEJAN
Department of Mechanical Engineering, Campus Box 427, University of Colorado, Boulder, CO 80309, U.S.A.

(*Received* 7 *April* 1982 *and in revised form* 22 *September* 1982)

Abstract—This numerical study documents the effect of internal flow obstructions on heat transfer through a 2-dim. porous layer heated from the side. Three types of flow obstructions have been considered. Horizontal diathermal partitions were found to decrease the heat transfer rate in cases where the overall heat transfer was dominated by convection. In the conduction-dominated regime, horizontal diathermal partitions were found to increase the heat transfer rate slightly. Horizontal adiabatic partitions, on the other hand, were found to increase the heat transfer rate when the dominating mechanism is convection. Finally, vertical diathermal partitions were shown to reduce the heat transfer rate by roughly 50% in the convection-dominated regime. Numerical heat transfer results are reported in the domain $0.1 < L/H < 2$ and $50 < Ra_H < 1000$, where L/H is the length/height ratio and Ra_H is the Darcy-modified Rayleigh number based on height.

NOMENCLATURE

c_p, fluid specific heat at constant pressure;
g, gravitational acceleration;
H, vertical dimension of the porous layer;
k, thermal conductivity of the fluid-saturated porous structure;
K, permeability;
l, length of horizontal partition (Fig. 1);
L, horizontal dimension of the porous layer;
Nu, conduction-based Nusselt number, equation (16);
Nu_a, Nusselt number of layer with horizontal adiabatic partition (Fig. 4);
Nu_d, Nusselt number for layer with horizontal diathermal partition (Fig. 4);
Nu_0, base Nusselt number, for layer without internal flow obstruction (Fig. 4);
Nu_v, Nusselt number for layer with vertical diathermal partition (Fig. 5);
P, pressure;
Ra_H, Rayleigh number based on H, equation (14);
Res, convergence criterion, equation (15);
T, temperature;
T_{cold}, temperature of cold vertical wall (Fig. 1);
T_{warm}, temperature of warm vertical wall (Fig. 1);
ΔT, overall temperature difference, $T_{warm} - T_{cold}$;
u, horizontal velocity component;
v, vertical velocity component;
x, horizontal coordinate;
y, vertical coordinate.

Greek symbols

α, thermal diffusivity, $k/(\rho c_p)$;
β, coefficient of thermal expansion;
μ, dynamic viscosity;
ν, kinematic viscosity;
ρ, fluid density;
ψ, stream function;
$(\,)_*$, dimensionless variables, equations (11).

INTRODUCTION

THE FLOW and heat transfer induced by buoyancy effects in a porous medium saturated with fluids has attracted considerable attention. Much of this work has been summarized in a comprehensive review by Cheng [1] who showed that the interest in this natural convection phenomenon is fueled by important engineering applications, for example, geothermal energy conversion and thermal insulation engineering. The latter is the heat transfer application which inspired the present study.

The basic model used so far in connection with porous insulations heated from the side, consists of a 2-dim. porous medium with vertical walls at different temperatures and with adiabatic top and bottom walls. The early experimental studies of Schneider [2], Mordchelles-Regnier *et al.* [3] and Klarsfeld [4] demonstrated that the net heat transfer rate across the porous layer increases monotonically as the Rayleigh number increases. These measurements were verified later by Bankvall [5]. Similar numerical results were obtained by Chan *et al.* [6] and Burns *et al.* [7]. The latter group documented also the effect of fluid leakage through the walls which contain the rectangular porous structure.

The theoretical work on the convection-dominated regime of porous layers heated from the side was pioneered by Weber [8] who developed an Oseen-linearized solution for the boundary layer regime in a tall layer ($H/L > 1$). The Weber solution was modified later by the present author, to account for the heat transfer taking place vertically through the core region of a moderately tall layer [9]. Simpkins and Blythe [10] reported an alternative theory for the boundary layer regime, based on a solution of the integral type [11]. The same authors extended their theory to the more general case where the fluid viscosity is sensitive to temperature variations [12]. Simpkins and Blythe [10] showed that the boundary layer theories of refs. [8–10] account satisfactorily for the heat transfer rates

reported experimentally and numerically for high Rayleigh numbers in tall layers.

A number of recent studies have shown that the natural convection pattern in a shallow layer ($H/L < 1$) can differ substantially from the pattern revealed by the study of tall layers. Walker and Homsy [13] developed an asymptotic solution for the flow and temperature fields, using the geometric ratio H/L as a small parameter. They showed that, unlike in tall layers, the core region plays an active role in the heat transfer process. An integral-type analytical solution for the same geometry was proposed by Bejan and Tien [14]. Most recently, the shallow geometry was the subject of an extensive numerical study by Hickox and Gartling [15] which showed that the patterns of streamlines and isotherms differ greatly from the corresponding patterns in tall layers.

The literature reviewed above demonstrates that the homogeneous model for a 2-dim. porous layer has been studied extensively. From a practical standpoint, however, it is worth noting that the results based on this simple model have limited applicability: there are many situations where the space to be filled by porous insulation is not truly 'empty', as there are situations where the porous insulation itself is not homogeneous. An example of a space which is not 'empty' is the double-wall space filled with fiberglass insulation in contemporary buildings: each side wall is reinforced on the inside with structural members which, if positioned horizontally, resemble the internal flow obstruction l shown in Fig. 1. An example of nonhomogeneous insulation material is the blanket of fiberglass insulation: the blanket is covered on one side with paper which, when more than one blanket is used, acts as an internal flow obstruction.

The objective of the present study is to document the heat transfer effect associated with the presence of flow obstructions inside a porous layer heated from the side.

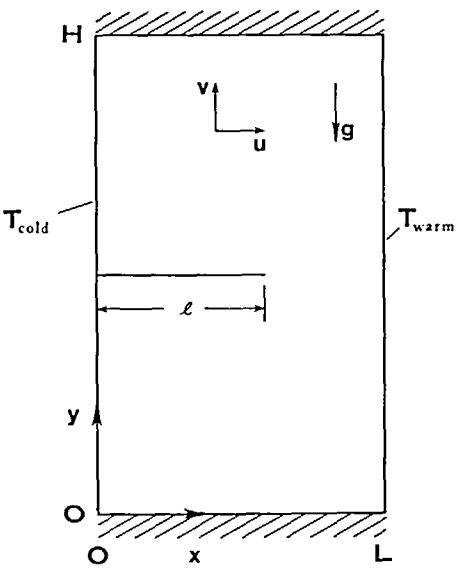

FIG. 1. Schematic of 2-dim. porous layer with horizontal diathermal flow obstruction.

MATHEMATICAL FORMULATION

The focus of the following analysis is on the 2-dim. rectangular space filled with porous material shown in Fig. 1. In accordance with the homogeneous porous medium model [16], the equations accounting for the conservation of mass, momentum and energy at any point (x, y) are

$$\frac{\partial u}{\partial x}+\frac{\partial v}{\partial y}=0, \tag{1}$$

$$u=-\frac{K}{\mu}\frac{\partial P}{\partial x}, \tag{2}$$

$$v=-\frac{K}{\mu}\left(\frac{\partial P}{\partial y}+\rho g\right), \tag{3}$$

$$u\frac{\partial T}{\partial x}+v\frac{\partial T}{\partial y}=\alpha\left(\frac{\partial^2 T}{\partial x^2}+\frac{\partial^2 T}{\partial y^2}\right). \tag{4}$$

In the above equations, u, v, μ, P, and T are the fluid velocity components (Fig. 1), the viscosity, the pressure and the temperature. The two momentum equations (2) and (3) reflect the Darcy flow model, where K stands for the permeability of the porous material. It is assumed that the fluid and the porous solid matrix are in *local* thermal equilibrium, at temperature $T(x, y)$. The thermal diffusivity α is defined as $\alpha = k/(\rho c_p)$: here, k is the thermal conductivity of the fluid-porous-matrix composite and (ρc_p) is the thermal capacity of the fluid alone.

The governing equations (1)–(4) reflect also the Boussinesq approximation, whereby the fluid density ρ is regarded as a constant except in the body force term of the vertical momentum equation (3) where it is replaced by

$$\rho=\rho_0[1-\beta(T-T_0)]. \tag{5}$$

Using this approximation, and eliminating the pressure terms between equations (2) and (3), yields a unique momentum conservation statement,

$$\frac{\partial u}{\partial y}-\frac{\partial v}{\partial x}=-\frac{Kg\beta}{\nu}\frac{\partial T}{\partial x}. \tag{6}$$

In equation (6), β and ν are the coefficient of thermal expansion and the kinematic viscosity μ/ρ_0.

The boundary conditions are the same as in the majority of the existing studies of porous layers heated from the side [5–15]

impermeable walls

$$\begin{aligned} u&=0 \quad \text{at} \quad x=0, L,\\ v&=0 \quad \text{at} \quad y=0, H, \end{aligned} \tag{7}$$

isothermal vertical walls

$$\begin{aligned} T&=T_{cold} \quad \text{at} \quad x=0,\\ T&=T_{warm} \quad \text{at} \quad x=L, \end{aligned} \tag{8}$$

adiabatic horizontal walls

$$\frac{\partial T}{\partial y}=0 \quad \text{at} \quad y=0, H. \tag{9}$$

However, in addition to these peripheral conditions, we take into account the new feature which constitutes the focus of the present study

partial flow obstruction (Fig. 1),

$$v = 0 \quad \text{at} \quad y = H/2, \quad 0 < x < l. \tag{10}$$

The obstruction is assumed to interfere only with the fluid circulation through the porous layer; in other words, the temperature difference from $y = (H/2)^+$ to $y = (H/2)^-$, across the obstruction, is assumed negligible. The heat transfer effect of the partial flow obstruction was evaluated numerically, as shown in the next section.

NUMERICAL SOLUTION

The mathematical problem formulated above was first placed in dimensionless form by defining the new dimensionless variables

$$x_* = x/L, \quad y_* = y/H,$$
$$\psi_* = \frac{\psi v}{Kg\beta L\Delta T}, \quad T_* = \frac{T - T_{\text{cold}}}{T_{\text{warm}} - T_{\text{cold}}} \tag{11}$$

where ψ is the streamfunction ($u = \partial\psi/\partial y$, $v = -\partial\psi/\partial x$) and $\Delta T = T_{\text{warm}} - T_{\text{cold}}$. The dimensionless forms of the momentum and energy equations are then

$$\frac{\partial^2\psi_*}{\partial x_*^2} + \left(\frac{L}{H}\right)^2 \frac{\partial^2\psi_*}{\partial y_*^2} = -\frac{\partial T_*}{\partial x_*}, \tag{12}$$

$$\left(\frac{L}{H}\right)^2 Ra_H \left(\frac{\partial\psi_*}{\partial y_*}\frac{\partial T_*}{\partial x_*} - \frac{\partial\psi_*}{\partial x_*}\frac{\partial T_*}{\partial y_*}\right) = \frac{\partial^2 T_*}{\partial x_*^2} + \left(\frac{L}{H}\right)^2 \frac{\partial^2 T_*}{\partial y_*^2} \tag{13}$$

where Ra_H is the Darcy-modified Rayleigh number

$$Ra_H = \frac{Kg\beta H\Delta T}{\alpha\nu}. \tag{14}$$

The corresponding dimensionless form of boundary conditions (7)–(10) is

$$\psi_* = 0 \quad \text{at} \quad x = 0, 1,$$
$$\text{at} \quad y = 0, 1,$$
$$\text{at} \quad y = 1/2 \text{ and } 0 < x < l/L,$$
$$T_* = 0 \quad \text{at} \quad x = 0,$$
$$T_* = 1 \quad \text{at} \quad x = 1,$$
$$\frac{\partial T_*}{\partial y_*} = 0 \quad \text{at} \quad y = 0, 1.$$

The present numerical solution was developed using the finite difference scheme employed earlier by Bankvall [5] in the study of natural convection in porous layers without internal flow obstructions. The choice of an already-used numerical scheme was intentional, in order to be able to check the validity of the present results against published results for the no-obstruction case ($l/L = 0$); this test is presented later in this section. Therefore, since no originality is claimed in the set-up of the numerical procedure, the reader is directed to ref. [5] for an outline of the finite difference approach.

The only unusual aspect of the present work is that it was performed on a personal computer (Apple II). Since personal computers are not widely used in the numerical solution of nonlinear heat transfer problems, the reader may be interested in how Apple II performed. A few details are offered below.

The finite-difference approximation of the governing equations was based on dividing the $0 \leqslant x_* \leqslant 1$ interval into N_x equal segments separated by $N_x + 1$ nodes. Likewise, the y_* interval was divided into N_y segments. As shown in ref. [5], the numerical work starts with postulating a certain distribution of flow and temperature in the $x_* - y_*$ space: in the present solution the 'start-up' distributions were taken as $\psi_* = 0$ and $T_* = x_*$, i.e. no flow and pure conduction. Based on these 'old' fields, the momentum equation (12) is used to determine point-by-point the new ψ_* field, while the energy equation (13) is used to determine the new T_* field. The new ψ_* and T_* are next relegated to the 'old' status and the calculation is repeated until the changes in ψ_* and T_* during one calculation (iteration) satisfy the convergence criterion

$$\left|\frac{\tau_{\text{new}} - \tau_{\text{old}}}{\tau_{\text{old}}}\right| \leqslant Res \tag{15}$$

at every point in the system. In criterion (15), τ stands for either ψ_* or T_*, while Res is a sufficiently small number chosen so that the Nusselt number change during one iteration is negligible [7].

Table 1 shows a sample of computational parameters noted in the course of solving the case $Ra_H = 400$, $L/H = 0.5$ and $l/L = 0$ (no obstruction). The duration of one iteration and the total number of iterations increase dramatically as the grid fineness is enhanced. The corresponding changes in the Nusselt number, defined by equation (16), are negligibly small if the grid is 12 × 12 or finer. The total computation time decreases sharply as the convergence criterion is relaxed, i.e. as Res increases. All the numerical solutions documented in this paper were obtained using the 20 × 20 grid and $Res = 10^{-5}$; it is worth noting that $Res = 10^{-5}$ is more stringent as a convergence criterion than the value

Table 1. Sample of computational parameters ($Ra_H = 400$, $L/H = 0.5$, $l/L = 0$)

Grid fineness $N_x \times N_y$	Res equation (15)	Time for one iteration (s)	Total number of iterations	Nu equation (16)
8 × 8	10^{-6}	11	69	4.807
12 × 12	10^{-6}	26	154	5.133
16 × 16	10^{-6}	46	352	5.175
20 × 20	10^{-6}	72	387	5.131
20 × 20	10^{-5}	72	136	5.210

Table 2. Comparison of the present results with previously published numerical heat transfer data for porous layers without internal flow obstructions ($l/L = 0$, $L/H = 2$)

Rayleigh number Ra_H	Nusselt number, equation (16)			
	Present study	Hickox and Gartling [15]	Bankvall [5]	Burns *et al.* [7]
25	1.397	1.410	~1.43*	~1.54*
50	2.213	2.155	~2.30*	~2.81*

* Values reported graphically by their original authors, hence approximate values given.

0.005 used in an earlier study of porous layers without internal flow obstructions [7]. Due to the low value chosen for *Res* and the fineness of the grid, the computation times required by the present study can be characterized as 'long'. However, 'speed' is no longer a deciding factor when a personal computer is being used.

To test the validity of the present heat transfer calculations, Table 2 shows a comparison with previously published Nusselt numbers for a porous layer without internal flow obstruction ($l/L = 0$, $L/H = 2$). Table 2 is an extension of the test used by Hickox and Gartling [15] to check the accuracy of their finite element scheme. It is clear that the present results agree well with the earlier data, especially with the earlier Nu's which have been reported in numerical form by their original authors (e.g. ref. [15]).

HEAT TRANSFER RESULTS

Figures 2 and 3 illustrate the flow and temperature patterns calculated numerically in order to determine the effect of the flow obstruction on heat transfer. The flow documented in Figs. 2 and 3 takes place in a moderately tall enclosure ($L/H = 0.5$) at the highest Rayleigh number permitted by the numerical scheme ($Ra_H = 400$): this case belongs to the "boundary layer regime" [8], because the vertical boundary layer thickness ($\sim H/Ra_H^{1/2}$) is ten times smaller than the horizontal dimension of the space (L). The streamline patterns plotted in Fig. 2 show that as the length of the lateral obstruction increases from $l/L = 0$ to $l/L = 0.5$ and, finally, to $l/L = 1$, the single cell is eventually divided into two cells. Most importantly, the flow obstruction has the effect of 'snuffing out' the circulation: the total flow rate decreases from $(\psi_*)_{max} = 0.060$ in the original no-obstruction case, to $(\psi_*)_{max} = 0.0388$ in the ultimate case where $l/L = 1$. As shown later in this section (Table 3), when the heat transfer rate is strongly dominated by convection, the slowing down of the counterclockwise circulation reflects in a decreasing Nusselt number. In other words, in the boundary layer regime the flow obstruction enhances the thermal insulation capability of the porous layer.

The pattern of isotherms displayed in Fig. 3 shows the distortion associated with the growth of the flow obstruction. The three patterns of Fig. 3 correspond on a one-to-one basis to the three streamline patterns shown in Fig. 2 ($l/L = 0, 0.5, 1$). The isotherms show that there is heat transfer through the flow obstruction, and that the direction of the heat transfer is *upward*.

The net heat transfer between the vertical walls of the porous layer was calculated for 70 different cases, covering the effect of changing L/H, Ra_H and l/L. Table 3 reports the Nusselt numbers resulting from these

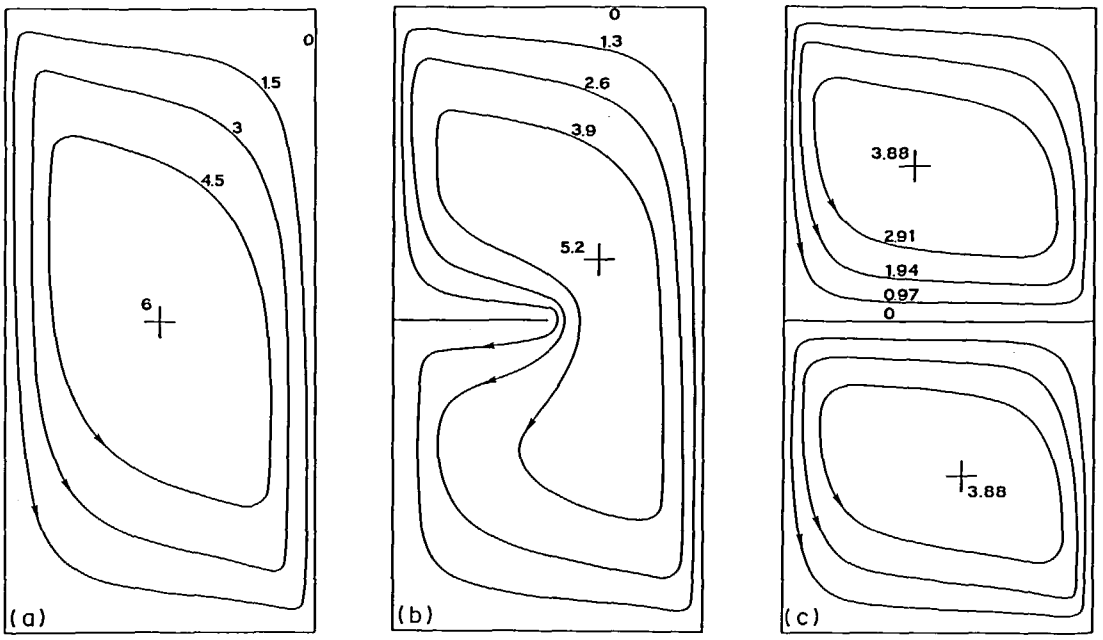

FIG. 2. Pattern of streamlines for $L/H = 0.5$, $Ra_H = 400$. (a) $l/L = 0$, (b) $l/L = 1/2$, (c) $l/L = 1$. (The numbers on the streamlines are the values of $100\,\psi_*$.)

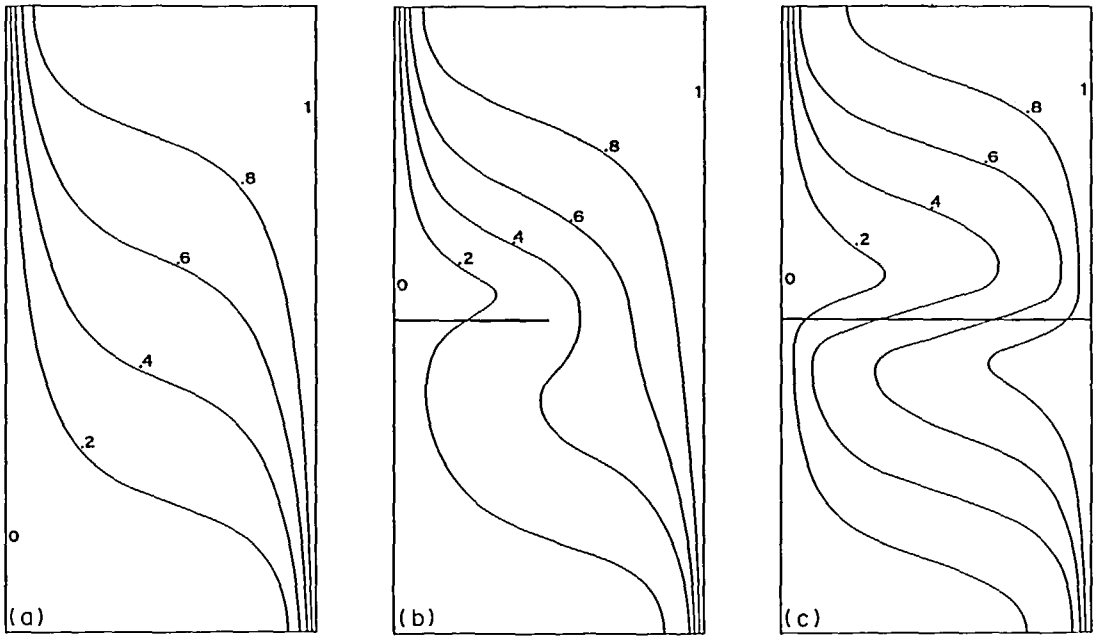

FIG. 3. Pattern of isotherms for $L/H = 0.5$, $Ra_H = 400$. (a) $l/L = 0$, (b) $l/L = 1/2$, (c) $l/L = 1$.

calculations: the Nusselt number is defined as

$$Nu = \frac{\text{net heat transfer}}{\text{pure conduction}} = \frac{k\int_0^H \left(\frac{\partial T}{\partial x}\right)_{x=0,L} \mathrm{d}y}{kH\Delta T/L}. \quad (16)$$

The flow obstruction causes significant reductions in the heat transfer rate as Ra_H increases and as L/H increases. For the (Ra_H, L/H) case documented in Figs. 2 and 3, for example, the heat transfer rate decreases by 13% as the obstruction grows to full length. In another case ($Ra_H = 200$, $L/H = 1$) the full growth of the flow obstruction causes a 44% drop in the overall heat transfer rate.

When pure conduction is still the dominant heat transfer mechanism, i.e. when Nu is of order one, the flow obstruction actually causes a *slight increase* in the heat transfer rate. This unexpected effect is present in tall layers and at moderately low Rayleigh numbers (Table 3). A possible explanation for this effect may be given based on the distortion of the isotherms (Fig. 3). When the heat transfer is conduction-dominated, the heated fluid travels through the entire porous structure (not through a thin wall layer, as in Fig. 2). Thus, when the lateral flow obstruction is present, the $L/2$-thick stream cooled by the left wall is pushed closer to the warm wall: although small, the convective heat transfer contribution is enhanced in this manner. In the boundary layer regime, on the other hand, the stream cooled by the left wall (the wall holding the obstruction) is much thinner than the opening left beyond the tip of the partition (see the middle streamline pattern in Fig. 2). Even when the obstruction severs the layer ($l/L = 1$), the stream cooled by the left wall reaches the warm wall *after* it was heated by its counterpart vertically through the obstruction.

To summarize, the obstruction deflects one stream (boundary layer) laterally. If the stream makes thermal contact with the opposite vertical wall, then the heat transfer is augmented; this is the case of wide streams (low Ra_H, $Nu \sim 1$). If the stream is narrow, then it will be heated by heat transfer through the partition, before it will come in contact with the heated vertical wall. Consequently, in the boundary layer regime (high Ra_H, $Nu > 1$) the heat transfer rate is not augmented by the stream-deflection mechanism.

Table 3. Summary of heat transfer results: the numbers represent the values of Nu defined by equation (16)

		l/L				
L/H	Ra_H	0	0.25	0.5	0.75	1
1	50	1.897	1.721	1.423	1.286	1.275
	100	3.433	2.855	2.273	1.914	1.876
	200	6.044	5.167	4.244	3.494	3.369
0.5	50	1.383	1.314	1.250	1.235	1.234
	100	2.023	1.884	1.729	1.688	1.688
	200	3.226	3.021	2.758	2.664	2.669
	400	5.210	4.950	4.617	4.507	4.556
0.25	50	1.052	1.054	1.062	1.067	1.068
	100	1.205	1.204	1.229	1.247	1.249
	200	1.607	1.587	1.633	1.703	1.708
	400	2.431	2.374	2.365	2.599	2.616
	800	3.807	3.724	3.628	*	*
0.1	250	1.069	1.076	1.092	1.099	1.100
	500	1.215	1.233	1.293	1.323	1.325
	1000	1.565	1.582	*	*	*

* In these cases the numerical solution did not converge.

THE EFFECT OF HEAT TRANSFER THROUGH THE HORIZONTAL FLOW OBSTRUCTION

In the numerical solutions discussed so far the horizontal flow obstruction was modeled as diathermal (perfect conductor in the y direction). In a real-life engineering system any flow obstruction will, at least in part, act as a thermal insulator as well. The purpose of this section is to document the Nu effect associated with modeling the horizontal obstruction as adiabatic.

The Nusselt number for a vertical porous layer severed in half by an impermeable and adiabatic partition can be deduced directly from Table 3. If the porous system of interest is described by $(L/H, Ra_H)$, then the same system partitioned by an adiabatic wall is equivalent to placing two $(L/(H/2), Ra_{H/2})$ systems on top of one another. For example, in the porous layer illustrated in Figs. 2 and 3 ($L/H = 0.5$, $Ra_H = 400$) the calculated Nusselt number is $Nu = 5.21$ (from Table 3, $l/L = 0$). Now, if the full-length partition is adiabatic, then each square half of the partitioned system is described by ($l/L = 0, L/H = 1, Ra_H = 200$): thus, from Table 3, the Nusselt number for the partitioned system is $Nu = 6.044$.

The above example is presented graphically in Fig. 4: the base Nusselt number for the system without flow obstruction is $Nu_0 = 5.21$, while for the case of a full-length adiabatic partition we have $Nu_a = 6.044$. The example is completed by adding the case where the full-length partition is diathermal: Table 3 for $L/H = 0.5$, $Ra_H = 400$, $l/H = 1$ yields $Nu_d = 4.556$.

The example of Fig. 4 illustrates vividly the heat transfer enhancement mechanism discussed as conclusion to the preceding section. When the flow obstruction is a good insulator, the cold boundary layer is brought (cold) in contact with the warm wall, and the heat transfer rate is enhanced ($Nu_a > Nu_0$). When the obstruction is a good thermal conductor, the cold boundary layer warms up before reaching the opposite warm wall and, as a result, the transfer of heat is inhibited ($Nu_d < Nu_0$).

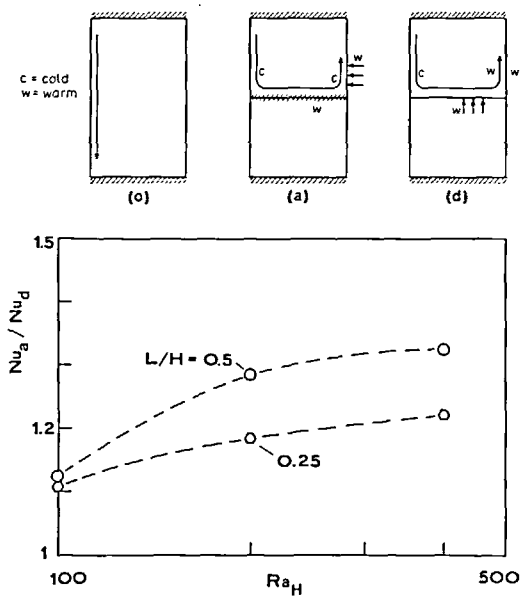

FIG. 4. The decrease in overall Nusselt number associated with heat transfer vertically through the partition; (a) no partition, 0; (b) adiabatic partition, a; (c) diathermal partition, d.

The important engineering conclusion of the above discussion is that the vertical heat transfer through the horizontal flow obstruction has a measurable thermal insulation effect, hence,

$$Nu_d < Nu_a. \tag{17}$$

The graph shown in the lower half of Fig. 4 enforces this conclusion, and shows that the discrepancy between Nu_a and Nu_d increases as both Ra_H and L/H increase.

It is worth commenting on the fact that both the single-cell flow of Fig. 4(a) and the two-cell partitioned flow of Fig. 4(c) satisfy the same *outer* boundary conditions, namely, isothermal vertical walls and adiabatic horizontal walls. Thus, Figs. 4(a) and (c) may suggest the existence of steady solutions which are not unique, in the medium defined by the outer boundaries. In this author's view, such an interpretation is incorrect since the flow of Fig. 4(c) cannot exist in the unpartitioned layer of Fig. 4(a), because it would exhibit a step change in horizontal velocity (this feature can only be associated with the presence of an internal impermeable partition).

THE THERMAL INSULATION EFFECT OF A VERTICAL DIATHERMAL PARTITION

The numerical scheme used to obtain the heat transfer results discussed so far, was easily adapted to calculate the heat transfer in a porous layer partitioned by a full-height diathermal wall (Fig. 5). The effect of a vertical internal partition on heat transfer is important in a number of engineering problems. For example, when double-wall spaces are filled with fiberglass insulation, in many cases the fiberglass insulation comes in a blanket with paper backing; when two or more blankets are used, the paper backing interferes with the circulation of air through the porous insulation. It is useful to know the size of the additional insulation effect provided by the vertical internal surface which interferes with the flow.

Table 4 summarizes the Nusselt number calculations Nu_v made for the system sketched in the upper half of Fig. 5. For orientation, Table 4 lists also the base Nusselt numbers Nu_0 for the case where the vertical

Table 4. The Nu reduction associated with a vertical diathermal partition: the numbers listed below represent the ratio Nu_v/Nu_0

	Ra_H			
L/H	50	100	200	400
0.5		1.134/2.023	1.445/3.226	2.193/5.210
1	1.217/1.897	1.677/3.433	2.696/6.044	
2	1.510/2.213	2.419/4.201	4.285/7.993	

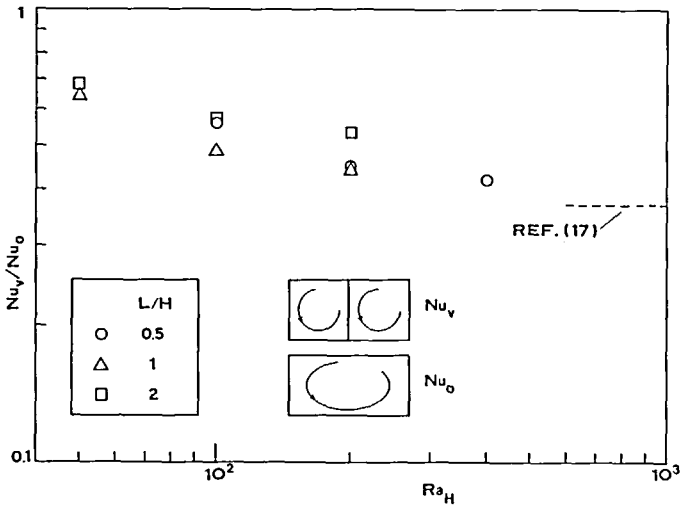

FIG. 5. The decrease in overall Nusselt number due to the presence of a vertical diathermal partition.

diathermal partition is absent. It is clear that as Ra_H increases, the vertical partition reduces the heat transfer rate to roughly half of the heat transfer rate in the same system without a partition. This conclusion is shown graphically in the lower half of Fig. 5: the ratio Nu_v/Nu_0 drops asymptotically to the '~37%' level predicted theoretically by Bejan and Anderson [17] from the study of natural convection on both sides of a diathermal wall imbedded in an infinite porous medium.

In conclusion, the presence of an impermeable vertical partition has a significant effect on reducing the net heat transfer rate through the porous layer.

CONCLUSIONS

This study determined numerically the effect of internal flow obstructions on heat transfer through a porous layer heated from the side. Three kinds of flow obstructions have been considered:

I. Horizontal diathermal partitions of variable length (Fig. 1).

II. Horizontal adiabatic partitions of full length (Fig. 4).

III. Vertical diathermal partitions of full height (Fig. 5).

The engineering conclusions reached in the case of each of these flow obstructions are:

I. When the heat transfer is dominated by convection, the heat transfer rate decreases steadily as the partition length increases (Table 3).
When the heat transfer is dominated by conduction, the heat transfer rate increases slightly as the partition length increases (Table 3).

II. When the horizontal partition is adiabatic, the heat transfer rate Nu_a is generally higher than the corresponding heat transfer rate when the partition is diathermal, Nu_d (Fig. 4).

The ratio Nu_a/Nu_d increases as both Ra_H and L/H increase.

III. A vertical diathermal partition reduces by about 50% the heat transfer rate in a convection-dominated porous layer (Table 4, Fig. 5).

The present numerical solutions are based on the Darcy flow model and, as such, they may not represent adequately the flow and temperature fields right next to the solid walls. The study of the true near-wall behavior would require an improved flow model to take into account the possible 'channelling' of fluid along the walls.

Acknowledgement—This work was supported in part by the National Science Foundation, through Grant No. MEA 82-07779.

REFERENCES

1. P. Cheng, Heat transfer in geothermal systems, *Adv. Heat Transfer* **14**, 1–105 (1979).
2. K. J. Schneider, Investigation of the influence of free thermal convection on heat transfer through granular material, *International Institute of Refrigeration, Proceedings*, pp. 247–253 (1963).
3. G. Mordchelles-Regnier, P. Micheau, A. Pirovano, C. Jumentier, J. S. Terpstra, Y. Lecourt, P. Cave and M. Breuille, Recherches recentes effectuees en France sur l'isolation thermique des reacteures nucleaires, International Atomic Energy Agency, Vienna, pp. 529–544 (1969).
4. S. Klarsfeld, Champs de temperature associes aux mouvements de convection naturelle dans un milieu poreux limite, *Rev. Gen. Thermique* **108**, 1403–1423 (1970).
5. C. G. Bankvall, Natural convection in vertical permeable space, *Wärme- und Stoffübertragung* **7**, 22–30 (1974).
6. B. K. C. Chan, C. M. Ivey and J. M. Barry, Natural convection in enclosed porous media with rectangular boundaries, *J. Heat Transfer* **92**, 21–27 (1970).
7. P. J. Burns, L. C. Chow and C. L. Tien, Convection in a vertical slot filled with porous insulation, *Int. J. Heat Mass Transfer* **20**, 919–926 (1977).
8. J. W. Weber, The boundary layer regime for convection in a vertical porous layer, *Int. J. Heat Mass Transfer* **18**, 569–573 (1975).

9. A. Bejan, On the boundary layer regime in a vertical enclosure filled with a porous medium, *Lett. Heat Mass Transfer* **6**, 93–102 (1979).
10. P. G. Simpkins and P. A. Blythe, Convection in a porous layer, *Int. J. Heat Mass Transfer* **23**, 881–887 (1980).
11. P. A. Blythe and P. G. Simpkins, Thermal convection in a rectangular cavity, in *Physicochemical Hydrodynamics*, Vol. 2, pp. 511–524, Advance, New York (1977).
12. P. A. Blythe and P. G. Simpkins, Convection in a porous layer for a temperature dependent viscosity, *Int. J. Heat Mass Transfer* **24**, 497–506 (1981).
13. K. L. Walker and G. M. Homsy, Convection in a porous cavity, *J. Fluid Mech.* **87**, 449–474 (1978).
14. A. Bejan and C. L. Tien, Natural convection in a horizontal porous medium subjected to an end-to-end temperature difference, *J. Heat Transfer* **100**, 191–198 (1978).
15. C. E. Hickox and D. K. Gartling, A numerical study of natural convection in a horizontal porous layer subjected to an end-to-end temperature difference, *J. Heat Transfer* **103**, 797–802 (1981).
16. J. W. Elder, Steady free convection in a porous medium heated from below, *J. Fluid Mech.* **27**, 29–48 (1966).
17. A. Bejan and R. Anderson, Heat transfer across a vertical impermeable partition imbedded in porous medium, *Int. J. Heat Mass Transfer* **24**, 1237–1245 (1981).

CONVECTION THERMIQUE NATURELLE DANS UNE COUCHE POREUSE AVEC DES OBSTRUCTIONS DE L'ECOULEMENT INTERNE

Résumé—Cette étude numérique concerne l'effet des obstructions de l'écoulement interne sur le transfert thermique à travers une couche poreuse bidimensionnelle chauffée latéralement. On considère trois types d'obstruction. Des partitions diathermales horizontales diminuent le taux de transfert thermique dans le cas où le transfert global est dominé par la convection. Dans le régime dominé par la conduction, les partitions diathermales horizontales augmentent légèrement le transfert thermique. Des partitions diathermales verticales réduisent le transfert thermique d'environ 50% dans le régime dominé par la convection. Des résultats numériques sont donnés dans le domaine $0{,}1 < L/H < 2$ et $50 < Ra_H < 1\,000$, où L/H est le rapport longueur/hauteur et Ra_H est le nombre de Rayleigh basé sur la hauteur et modifié au sens Darcy.

WÄRMEÜBERTRAGUNG DURCH FREIE KONVEKTION IN EINER PORÖSEN SCHICHT MIT INTERNEN STRÖMUNGSHINDERNISSEN

Zusammenfassung—Diese numerische Studie belegt den Einfluß von internen Strömungshindernissen auf die Wärmeübertragung durch eine von der Seite beheizte, zweidimensionale poröse Schicht. Drei Arten von Strömungshindernissen wurden berücksichtigt. Es wurde festgestellt, daß horizontale, diatherme Unterteilung den Wärmedurchgang vermindert, wenn der Wärmetransport durch Konvektion beherrscht wird. Wenn Wärmeleitung vorherrscht, wird durch horizontale, diatherme Unterteilung der Wärmedurchgang leicht verbessert. Horizontale, adiabate Unterteilung vergrößert andererseits den Wärmedurchgang, wenn Konvektion der vorherrschende Mechanismus ist. Schließlich und endlich wird gezeigt, daß senkrechte, diatherme Unterteilung den Wärmedurchgang im durch Konvektion dominierten Zustand um rund 50% vermindert. Numerische Wärmedurchgangs-Ergebnisse werden für die Bereiche $0{,}1 < L/H < 2$ und $50 < Ra_H < 1000$ mitgeteilt, wobei L/H das Längen-Höhen-Verhältnis und Ra_H die nach Darcy modifizierte, auf die Höhe bezogene Rayleigh-Zahl ist.

ТЕПЛОПЕРЕНОС ЕСТЕСТВЕННОЙ КОНВЕКЦИЕЙ В ПОРИСТОМ СЛОЕ С ВНУТРЕННИМИ ПЕРЕГОРОДКАМИ

Аннотация—Проведено численное исследование влияния внутренних перегородок на теплоперенос в нагреваемом сбоку двумерном пористом слое. Рассмотрены три типа перегородок. Найдено, что горизонтальные диатермические разделительные перегородки снижают интенсивность теплопереноса в случаях, когда в суммарном теплопереносе преобладает конвективная составляющая. В режиме с преобладанием теплопроводности такие перегородки приводят к некоторой интенсификации теплопереноса. С другой стороны, адиабатические перегородки приводят к увеличению плотности теплового потока, когда преобладающим механизмом является конвекция. Наконец, показано, что в режиме с преобладающей конвекцией вертикальные диатермические перегородки снижают интенсивность теплопереноса примерно на 50%. Численные результаты по теплопереносу представлены для диапазонов $0{,}1 < L/H < 2$ и $50 < Ra_H < 1000$, где L/H — отношение длины к высоте, а Ra_H — модифицированное число Рэлея с учетом закона Дарси.